

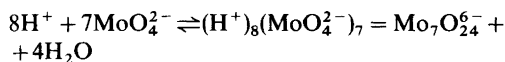
## On the Formation of Hepta- and Octamolybdates in Aqueous Solution. X-Ray Scattering and Raman Measurements

GEORG JOHANSSON,<sup>a</sup> LAGE PETTERSSON<sup>b</sup> and NILS INGRI<sup>b</sup>

<sup>a</sup> Department of Inorganic Chemistry, Royal Institute of Technology, S-100 44 Stockholm 70, Sweden and <sup>b</sup> Department of Inorganic Chemistry, University of Umeå, S-90187 Umeå, Sweden

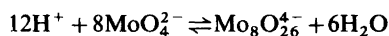
X-Ray scattering measurements have been performed on a series of 2.00 M lithium molybdate solutions with acidities ranging from  $Z=0$  to  $Z=1.50$ , where  $Z$  is the average number of protons consumed by each  $\text{MoO}_4^{2-}$  in the protolysis reactions. The scattering data are shown to be consistent with tetrahedral  $\text{MoO}_4^{2-}$  units in solutions with  $Z=0$  and with a dominant polymolybdate species having the  $\text{Mo}_7\text{O}_{24}^{6-}$  structure in solutions with  $Z=8/7=1.14$ . Observed changes in the radial distribution curves when  $Z$  increases from 1.14 to 1.50 indicate a partial transformation of the heptamolybdate species into a polymolybdate with a different structure. The observed changes are shown to be related to what would be expected if this species was identical with the Lindqvist octamolybdate ion,  $\text{Mo}_8\text{O}_{26}^{4-}$ , which has previously been found as discrete units in crystals. Recorded Raman spectra of the acidified solutions support these observations.

The complexes formed on acidification of an aqueous molybdate solution have been the subject of a large number of investigations. Several surveys of the literature have been given.<sup>1–4</sup> There seems to be general agreement on the occurrence of tetrahedral  $\text{MoO}_4^{2-}$  in alkaline solutions. Precise emf measurements, especially the fundamental studies by Sasaki and Sillén,<sup>2</sup> have established that the first species formed on acidification is a heptamolybdate:



This (8,7) complex, for which the number of protons consumed per  $\text{MoO}_4^{2-}$  is  $Z=8/7=1.14$ , has, by

Raman spectra<sup>1,5–7</sup> and by large-angle X-ray scattering measurements,<sup>8</sup> been shown to have the same structure as the discrete  $\text{Mo}_7\text{O}_{24}^{6-}$  anions found in several crystals<sup>9–11</sup> (Fig. 1). The species formed on further acidification ( $Z>1.14$ ) do not, however, seem to have been definitely established. Originally, Lindqvist<sup>12</sup> concluded that the next complex formed is an octamolybdate:



The structure of this (12,8) complex, for which  $Z=12/8=1.50$ , was assumed to be the same as that of the discrete  $\text{Mo}_8\text{O}_{26}^{4-}$  anions found in crystals of  $(\text{NH}_4)_4\text{Mo}_8\text{O}_{26}\cdot 5\text{H}_2\text{O}$ .<sup>12</sup> The structure of the  $\text{Mo}_8\text{O}_{26}^{4-}$  anions, first determined by Lindqvist,<sup>12</sup> has later been confirmed and refined by Gatehouse

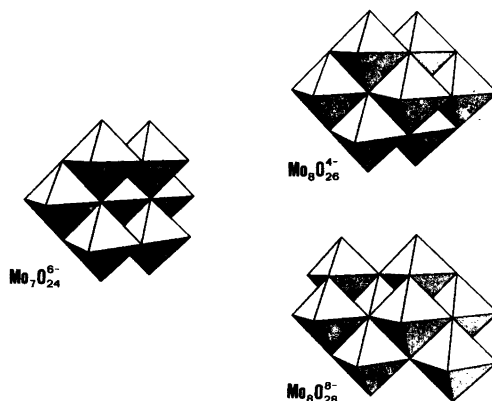


Fig. 1. The structures of hepta- and octamolybdate complexes found in crystals.  $\text{Mo}_7\text{O}_{24}$  and  $\text{Mo}_8\text{O}_{26}$  have been found to occur as discrete units. The  $\text{Mo}_8\text{O}_{28}$  groups are joined into infinite chains.<sup>22</sup>

in a structure determination of crystals of  $(\text{NH}_4)_4\text{Mo}_8\text{O}_{26}\cdot 4\text{H}_2\text{O}$ <sup>13</sup> (Fig. 1).

Attempts to analyze, by precise emf measurements, the equilibria occurring in the region between  $Z=1.14$  and  $Z=1.50$  have not, however, led to definite conclusions about the complexes formed. Emf data seem to be as equally well explained by a series of protonized heptamolybdate species as by a mixture of protonized hepta- and octamolybdates.<sup>14</sup> Attempts to identify, by means of Raman spectra, the complexes in solutions having  $Z=1.50$  with the octamolybdates in the crystals are less conclusive than the corresponding identification of the heptamolybdate.<sup>1,5,6</sup>

A structural change in the molybdate complexes, when  $Z$  is increased from 1.14 to 1.50, could possibly be established by measuring the X-ray scattering from a series of solutions with compositions within this region. A major structural change would not be expected if only protonized species of the heptamolybdate were formed. Although most emf investigations of the equilibria have been performed in ionic media containing sodium ions, lithium was chosen for the X-ray scattering measurements, as this allows the preparation of more concentrated solutions for  $Z > 1.14$ . Recent emf data, obtained in a 3.00 M lithium perchlorate medium,<sup>15</sup> indicate that although the complex formation starts at somewhat higher acidities the set of complexes formed is closely similar to that in sodium perchlorate medium.

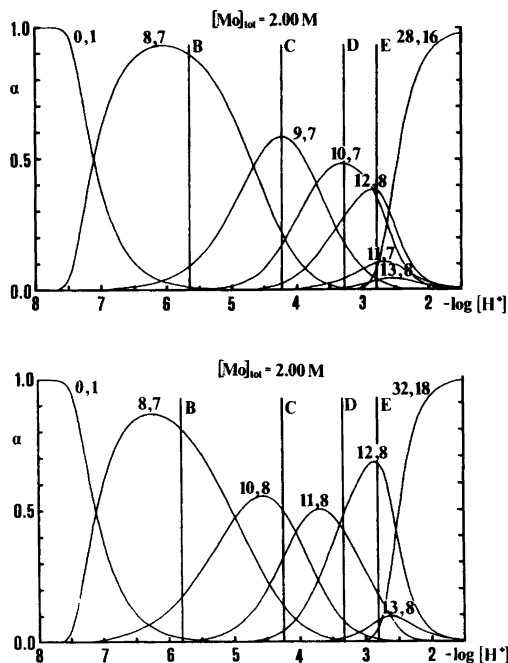


Fig. 2. The fraction,  $\alpha$ , of molybdenum bound in different species in a 2.00 M molybdate solution as a function of  $-\log [\text{H}^+]$ . The compositions of the solutions used for X-ray scattering measurements are marked by vertical lines. The two diagrams are calculated from two sets of constants, which both give an acceptable explanation of the emf data in 3.0 M  $\text{LiClO}_4$  medium.<sup>15</sup>

Table 1. Compositions of solutions.

	A $Z=0$	B $Z=1.14$	C $Z=1.29$	D $Z=1.43$	E $Z=1.50$
Concentrations in mol/l					
Mo	2.000	2.000	2.000	2.000	1.998
Li	4.000	1.714	1.429	1.143	1.000
O	58.9	59.2	58.9	58.6	58.6
H	101.8	104.6	104.4	104.1	101.2
Number of atoms in the chosen stoichiometric unit of volume, $V$					
Mo	1	1	1	1	1
Li	2.000	0.857	0.715	0.572	0.501
O	29.5	29.6	29.5	29.3	29.3
H	50.9	52.3	52.2	52.0	50.6
$V/\text{\AA}^3$	830.3	830.3	830.3	830.3	831.1
$\rho_0/e\text{\AA}^{-3}$	133.9	133.1	131.9	130.3	129.1

## EXPERIMENTAL

The compositions of the 2.00 M solutions used for the scattering measurements are given in Table 1. In Fig. 2 these compositions are indicated by vertical lines in diagrams giving the fraction of Mo bound in different complexes as a function of  $-\log[H^+]$ , as calculated from stability constants derived from emf data in a 3.00 M  $\text{LiClO}_4$  medium.<sup>15</sup> Results are given for two different sets of constants, one including predominantly hepta- and the other octamolybdates, but both giving satisfactory agreement between observed and calculated emf data.<sup>15</sup>

*Preparation of solutions.* Solution A ( $Z=0$ ) was prepared by dissolving  $\text{Li}_2\text{MoO}_4$  (Ventron *p.a.*) in water. Solutions B, C, D, and E ( $Z=1.14, 1.29, 1.43, 1.50$ ) were prepared by adding water to weighed amounts of  $\text{MoO}_3$  (Merck *p.a.*) and  $\text{Li}_2\text{CO}_3$  (Merck *p.a.*) and heating on a water bath until all solid phases were dissolved (in solution E a very small residue was filtered off). Finally a stream of  $\text{N}_2$  was bubbled through the solutions to remove dissolved  $\text{CO}_2$ .

*Scattering measurements.* The measurement of the X-ray scattering and the treatment of the intensity data were done in the way described in previous papers.<sup>8,16-18</sup>  $\text{AgK}\alpha$  radiation ( $\lambda=0.5608 \text{ \AA}$ ) was used. The measured intensities were normalized to a stoichiometric unit of volume corresponding to the average volume of one Mo atom in the solution. Scattering factors,  $f_i$ , and values for incoherent scattering were taken from the same sources as in previous works.

The reduced intensity values were calculated according to the expression  $i(s) = KI(s) - \sum f_i^2$ , where  $K$  is a normalization constant,  $I(s)$  are the observed intensity values,  $s = 4\pi \lambda^{-1} \sin \theta$ , and the summation in the last term is taken over all atoms in the stoichiometric unit of volume.<sup>18</sup> The radial distribution functions were calculated as

$$D(r) = 4\pi r^2 \rho_0 + (2r/\pi) \int_0^{s_{\max}} s(s)M(s) \sin(rs) ds,$$

with  $M(s) = f_{\text{Mo}}^2(0)/f_{\text{Mo}}^2(s) \exp(-0.01s^2)$ .<sup>18</sup> The functions  $D(r) - 4\pi r^2 \rho_0$  are shown in Fig. 3.

*Raman measurements.* Spectra were recorded with a Cary Model 82 Raman Spectrophotometer equipped with a Coherent Radiation 52B ion laser. The blue argon line at 488.0 nm was used for excitation. The measurements were performed at the Lipid Chemistry Laboratory, University of Gothenburg. For the liquid samples a wide cup with flat bottom, holding about 1–2 ml solution was used. The cup was placed to allow the laser beam to enter through the bottom, very close to the wall that turned towards the spectrophotometer slit, but avoiding reflection against the wall. With this technique the

pathway and, therefore, the absorption of the scattered Raman light was reduced to a minimum. The powdered  $\text{Na}_6\text{Mo}_7\text{O}_{24}(\text{H}_2\text{O})_{14}$  crystals were pressed in a conical cup coated with a wax to prevent parts of the sample falling down and contaminating the reflecting device.

## ANALYSIS OF DATA

*Scattering measurements.* For comparison with the observed radial distribution functions peak shapes<sup>18</sup> were calculated for the following complexes:  $\text{Li}(\text{H}_2\text{O})_4^+$ ,  $\text{MoO}_4^{2-}$ ,  $\text{Mo}_7\text{O}_{24}^{6-}$ , and  $\text{H}_2\text{O}$ . The hydrated lithium ion was assumed to form a regular tetrahedron with an  $\text{Li}-\text{H}_2\text{O}$  distance of 2.0  $\text{\AA}$  and with temperature coefficients,  $b$ ,<sup>18</sup> of 0.03  $\text{\AA}^2$  for  $\text{Li}-\text{H}_2\text{O}$  and 0.06  $\text{\AA}^2$  for  $\text{H}_2\text{O}-\text{H}_2\text{O}$ . These values were taken from an investigation of aqueous lithium chloride solutions by Narten *et al.*<sup>19</sup> For  $\text{Mo}_7\text{O}_{24}^{6-}$  the crystal structure parameters given by Sjöbom and Hedman<sup>10</sup> were used without modification. The temperature coefficients were arbitrarily chosen to be 0.002  $\text{\AA}^2$  for  $\text{Mo}-\text{Mo}$ , 0.004  $\text{\AA}^2$  for  $\text{Mo}-\text{O}$ , and 0.006  $\text{\AA}^2$  for  $\text{O}-\text{O}$  interactions. For  $\text{MoO}_4^{2-}$  a regular tetrahedral arrangement was assumed with an  $\text{Mo}-\text{O}$  distance of 1.77  $\text{\AA}$  and a temperature coefficient of 0.003  $\text{\AA}^2$ , in agreement with values found in the crystal structure determination of  $\text{Na}_2\text{MoO}_4 \cdot 2\text{H}_2\text{O}$  by Matsumoto *et al.*<sup>20</sup> and in a previous investigation of molybdate solutions.<sup>8</sup>

The results of the calculations are shown in Fig. 3, which gives a comparison with the observed distribution functions. A tetrahedral  $\text{MoO}_4^{2-}$  ion is consistent with the distribution function for solution A. The peaks that remain after subtracting the calculated peak shapes occur at distances which can reasonably be related to intermolecular distances in the solution. Similar results were obtained in an investigation reported in a previous paper.<sup>8</sup>

For solution B, which according to both schemes for the distribution of complexes given in Fig. 2 should contain most of the molybdenum bound in  $\text{Mo}_7\text{O}_{24}$  groups, the calculated shape function for an  $\text{Mo}_7\text{O}_{24}^{6-}$  complex is consistent with the distribution curve (Fig. 3). Subtraction of the calculated function leads to remaining peaks at about 3, 4.5, and 7  $\text{\AA}$ , that is, at distances corresponding to those observed for solution A. This, also, is in agreement with a previous investigation using solutions of

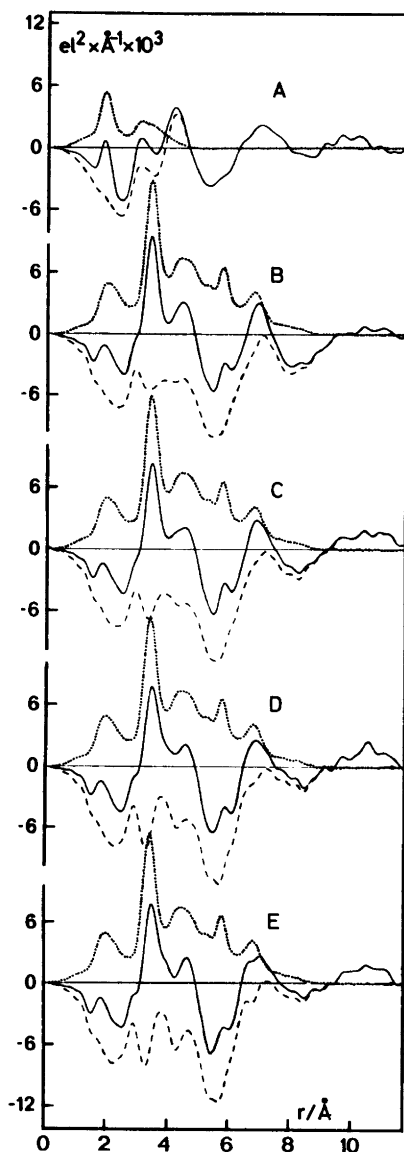


Fig. 3. Comparison between the experimental  $D(r) - 4\pi r^2 \rho_0$  functions (solid lines) and calculated shape functions (dotted lines), assuming all molybdenum to be bound in tetrahedral  $\text{MoO}_4^{2-}$  (solution A) or in  $\text{Mo}_7\text{O}_{24}$  complexes (solutions B to E), and lithium to form tetrahedral aqua complexes  $\text{Li}(\text{H}_2\text{O})_4^+$ . Dashed lines represent differences between observed and calculated functions.

slightly different compositions.<sup>8</sup>

For the more acid solutions C, D, and E, the agreement between the calculated shape function, assuming only  $\text{Mo}_7\text{O}_{24}$  groups occur, and the distribution functions becomes gradually worse with increasing  $Z$  value, which can be clearly observed in Fig. 3. The deviations seem too large to be explained only by different degrees of protonation of the  $\text{Mo}_7\text{O}_{24}^{6-}$  ion or by changes in its association with counter ions or water molecules.

The changes that take place can be more clearly demonstrated in the following way, which makes use of a method, described in a previous paper,<sup>21</sup> for the derivation of the shape function of a complex in a solution with the use of a reference solution of similar composition containing complexes of known structure. Using solution B, known to contain  $\text{Mo}_7\text{O}_{24}^{6-}$  complexes, as the reference, the results

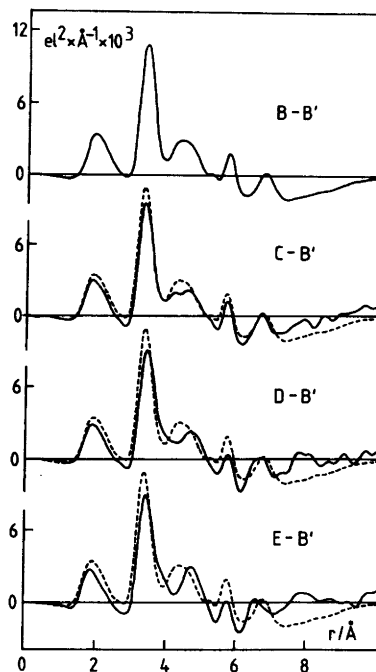


Fig. 4. The shape functions for the polymolybdate complexes in the solutions C, D, and E (solid lines) derived with the use of the solution B as the reference solution according to a method described in a previous paper.<sup>21</sup> The shape function for the  $\text{Mo}_7\text{O}_{24}$  complex (B - B'), as calculated from crystal structure parameters, is given for comparison (dashed lines).

given in Fig. 4 are obtained. The parameters used for the calculations were those given above, assuming the radii of the complexes to be 2.9 Å for  $\text{Li}(\text{H}_2\text{O})_4^+$ , 6.0 Å for  $\text{Mo}_7\text{O}_{24}^{6-}$ , and 1.8 Å for  $\text{H}_2\text{O}$ .

For solution B the resulting curve (B–B' in Fig. 4) will be the shape function for an  $\text{Mo}_7\text{O}_{24}^{6-}$  complex, calculated with the parameters given above and assumed to occupy a spherical hole of radius  $R=6.0$  Å in an evenly distributed electron density. For comparison, this shape function is plotted in Fig. 4 together with the derived shape function for each of the solutions C, D, and E. The differences observed will be caused by changes in the structures of the molybdenum complexes and also by changes in the packing of the complexes in the solution relative to those in the reference solution. Because of the similarities between the solutions the differences in intermolecular interactions should be small and, when they occur, should be expected only to lead to diffuse changes in the distribution curves. We will therefore assume in the following, that the localized changes in the distribution curves, observed in Figs. 3 and 4, will be due primarily to changes in the structures of the molybdate complexes.

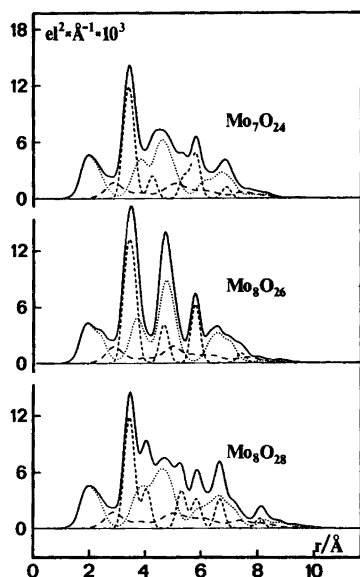


Fig. 5. Shape functions calculated from the crystal structure parameters for the  $\text{Mo}_7\text{O}_{24}$ ,  $\text{Mo}_8\text{O}_{26}$  and  $\text{Mo}_8\text{O}_{28}$  groups. The separate contributions from Mo–Mo distances (short dashes), Mo–O distances (dots), and O–O distances (long dashes) are shown.

In order to relate the observed differences to specific intramolecular interactions in the heptamolybdate structure, the calculated shape function of the  $\text{Mo}_7\text{O}_{24}^{6-}$  complex and the separate contributions from Mo–Mo, Mo–O, and O–O distances in the structure are given in Fig. 5. For comparison, the corresponding shape function for Lindqvist's octamolybdate,  $\text{Mo}_8\text{O}_{26}^{4-}$ , (Fig. 1) and for another octamolybdate,  $\text{Mo}_8\text{O}_{28}^{2-}$  (Fig. 1), derived from the molybdenum arrangement in the crystal structure of  $(\text{NH}_4)_6\text{Mo}_8\text{O}_{27}\cdot 4\text{H}_2\text{O}$ ,<sup>22</sup> are given. Differences between these shape functions are primarily due to differences in contributions from the Mo–Mo interactions. The O–O contributions are practically identical and the Mo–O contributions are similar. For a more direct comparison with the derived functions in Fig. 4, these molecular shape functions are given in Fig. 6 after including intermolecular interactions approximated by an even electron density outside a sphere surrounding the complex.

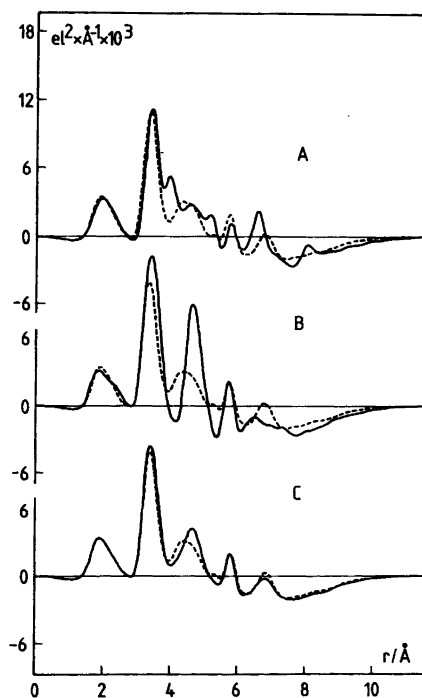


Fig. 6. Comparisons between calculated shape functions for the heptamolybdate  $\text{Mo}_7\text{O}_{24}^{6-}$  (dashed line) and  $\text{Mo}_8\text{O}_{28}$  (A),  $\text{Mo}_8\text{O}_{26}$  (B), and  $\text{Mo}_8\text{O}_{26} + \text{Mo}_7\text{O}_{24}$  in the ratio 1:3 (C).

A comparison between Figs. 4 and 6 shows the changes in the derived shape functions, when  $Z$  is increased (Fig. 4), to be related to those that would be expected if part of the heptamolybdate species were converted into complexes with the  $\text{Mo}_8\text{O}_{26}$  structure. No such direct relation is obvious for the other octamolybdate,  $\text{Mo}_8\text{O}_{28}$  (Fig. 6). The calculated shape function for an assumed mixture of complexes consisting of  $\text{Mo}_7\text{O}_{24}$  and  $\text{Mo}_8\text{O}_{26}$  units in the ratio 3:1, when compared with the  $\text{Mo}_7\text{O}_{24}$  function (Fig. 6, C), reproduces fairly well the difference observed between the solutions E and B (E - B' in Fig. 4).

A direct comparison between the  $D(r) - 4\pi r^2 \rho_0$  function for the solution E and the calculated shape functions leads to similar conclusions (Fig. 7).

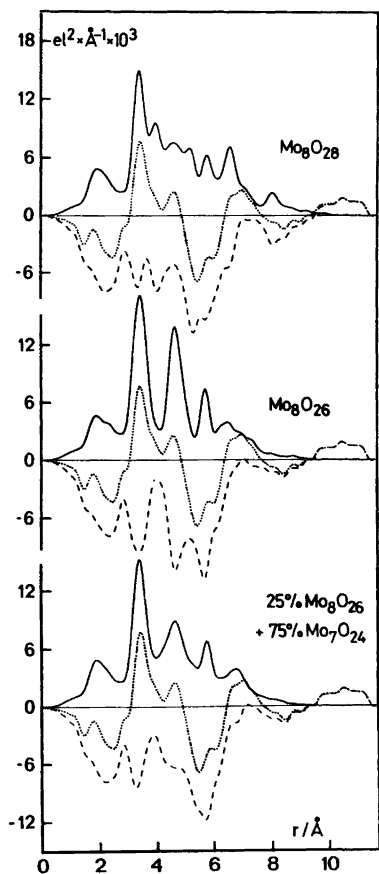


Fig. 7. The experimental radial distribution function for solution E (dotted lines) compared with calculated shape functions (solid lines). Differences between the functions are given by dashed lines.

The octamolybdate  $\text{Mo}_8\text{O}_{26}^{4-}$ , with the structure shown in Fig. 1, has a  $Z$  value of  $12/8 = 1.50$  and cannot be deprotonized. Octamolybdate species (10,8) and (11,8) included in the second set of stability constants used for the calculation of the distribution curves in Fig. 2 cannot, therefore, have this structure. According to the first set of constants used for the diagrams in Fig. 2, the less protonized

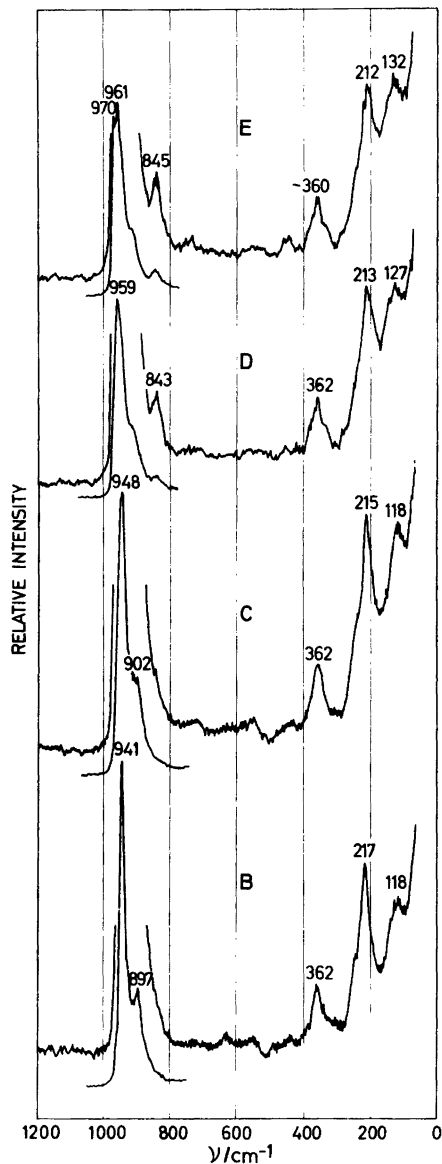


Fig. 8. Raman spectra of the acidified solutions B, C, D and E.

octamolybdates are not present. On the other hand, these constants lead to a range of existence of the (12,8) complex which should make its concentration in solution C negligible. The changes in the radial distribution curves, assumed to be caused by the formation of the (12,8) complex, are, however, clearly observable already for solution C.

**Raman data.** For the solutions B, C, D and E the Raman spectra were recorded and are shown in Fig. 8. The differences between the spectra when going from B ( $Z = 1.14$ ) to E ( $Z = 1.50$ ) are too large to be caused solely by a protonation reaction and indicate a structural change in the polymolybdate species.

The Raman spectrum of a solution with the same  $Z$  value as that of B, but with  $\text{Li}^+$  replaced by  $\text{Na}^+$  does not differ significantly from the spectrum of the solution B. It is compared in Fig. 9 with the spectrum taken of powdered  $\text{Na}_6\text{Mo}_7\text{O}_{24}(\text{H}_2\text{O})_{14}$  crystals, which contain discrete  $\text{Mo}_7\text{O}_{24}^{6-}$  ions. The main features of these two spectra are the same apart from the expected broadening of the peaks in

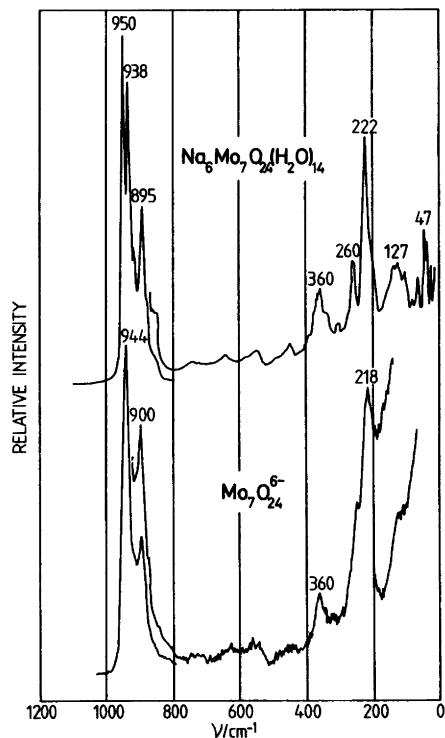


Fig. 9. Raman spectra of the solid phase  $\text{Na}_6\text{Mo}_7\text{O}_{24}(\text{H}_2\text{O})_{14}$  and of a sodium molybdate solution with  $[\text{Mo}^{\text{VI}}]_{\text{tot}} = 0.50 \text{ M}$ ,  $Z = 1.14$ .

Acta Chem. Scand. A 33 (1979) No. 4

the spectrum taken of the solution, resulting in a single peak at  $944 \text{ cm}^{-1}$ , which in the spectrum of the crystals is resolved into two separate peaks at  $938$  and  $950 \text{ cm}^{-1}$ . The Raman spectra thus strongly support the results of the scattering measurements, that the predominant complex in solution B is the heptamolybdate anion,  $\text{Mo}_7\text{O}_{24}^{6-}$ , with the structure determined from single crystal investigations<sup>9-11</sup> (Fig. 1). The spectrum of solution C ( $Z = 1.29$ ) has the same main features as that of solution B. No new peaks appear and the  $\text{Mo}_7\text{O}_{24}$  unit must still be predominant. However, in the spectra of solutions D ( $Z = 1.43$ ) and E ( $Z = 1.50$ ) a considerable displacement of some of the peaks has taken place and a new peak appears at  $844 \text{ cm}^{-1}$ . Aveston *et al.*<sup>1</sup> have reported the spectrum of the crystalline phase  $(\text{NH}_4)_4\text{MoO}_{26} \cdot 4\text{H}_2\text{O}$  known to contain discrete  $\text{Mo}_8\text{O}_{26}^{4-}$  anions.<sup>13</sup> This spectrum shows similarities to those of solutions D and E. For example, the most intense peak at  $963 \text{ cm}^{-1}$  and the two peaks at  $130$  and  $850 \text{ cm}^{-1}$  in the solid sample, correspond to the  $961$ ,  $132$  and  $845 \text{ cm}^{-1}$  peaks in solution E.

## CONCLUSIONS

The investigation shows that the heptamolybdate species present in solutions with  $Z = 1.14$  are partially transformed into at least one new polymolybdate, when  $Z$  is increased to  $1.50$ . The structure of this — or these — new species cannot be uniquely determined from the limited information contained in the solution diffraction data. A comparison of the observed changes in the radial distribution curves with expected changes for a formation of two different octamolybdate species (Fig. 1), known from crystal structure determinations, shows, however, that the formation of one of them,  $\text{Mo}_8\text{O}_{26}^{4-}$  (Fig. 1), can explain most of the changes observed. Raman spectra of the solutions support this interpretation.

**Acknowledgements.** The work has been supported by the Swedish Natural Science Research Council. We wish to thank ing. Ernst Hansen for skilful technical assistance and Professor Kåre Larsson, Gothenburg (now Lund), for kindly having placed the Raman spectrophotometer at our disposal.

## REFERENCES

1. Aveston, J., Anacker, E. W. and Johnson, J. *Inorg. Chem.* 3 (1964) 735.
2. Sasaki, Y. and Sillén, L. G. *Ark. Kemi* 29 (1968) 253.

3. Tsigdinos, G. A. *Bulletin Cdb-12a*, Climax Molybdenum Co., Greenwich, Conn. 1969.
4. Tytko, K.-H. and Glemser, O. *Adv. Inorg. Chem. Radiochem.* 19 (1976) 239.
5. Schönfeld, B. *Untersuchungen an wässrigen Isopolymolybdatlösungen*, Diss., Göttingen 1973.
6. Tytko, K.-H. and Schönfeld, B. *Z. Naturforsch. Teil B* 30 (1975) 471.
7. Lyhamn, L. and Pettersson, L. *Chem. Scr.* 20 (1979) 142.
8. Johansson, G., Pettersson, L. and Ingri, N. *Acta Chem. Scand. A* 28 (1974) 1119.
9. Lindqvist, I. *Ark. Kemi* 2 (1950) 325.
10. Sjöbom, K. and Hedman, B. *Acta Chem. Scand.* 27 (1973) 3673.
11. Evans, H. T., Jr., Gatehouse, B. M. and Leverett, P. *J. Chem. Soc. Dalton Trans.* (1975) 505.
12. Lindqvist, I. *Ark. Kemi* 2 (1950) 349.
13. Gatehouse, B. M. *J. Less-Common Met.* 54 (1977) 283.
14. Sillén, L. G. *Pure Appl. Chem.* 17 (1968) 55.
15. Wennerholm, H. *Personal communication*.
16. Johansson, G. *Acta Chem. Scand.* 25 (1971) 2787; 20 (1966) 553.
17. Pocev, S. and Johansson, G. *Acta Chem. Scand.* 27 (1973) 2146.
18. Johansson, G. and Sandström, M. *Chem. Scr.* 4 (1973) 195.
19. Narten, A. H., Raslow, F. and Levy, H. A. *J. Chem. Phys.* 58 (1973) 5017.
20. Matsumoto, K., Kobayashi, A. and Sasaki, Y. *Bull. Chem. Soc. Jpn.* 48 (1975) 1009.
21. Johansson, G., Pettersson, L. and Ingri, N. *Acta Chem. Scand. A* 32 (1978) 407.
22. Bösch, I., Buss, B. and Krebs, B. *Acta Crystallogr. B* 30 (1974) 48.

Received October 23, 1978.